Visual Acuity Modeling Using Optical Raytracing of Schematic Eyes

JOHN E. GREIVENKAMP, PH.D., JIM SCHWIEGERLING, M.S., JOSEPH M. MILLER, M.D., AND MARK D. MELLINGER, M.S.

• PURPOSE: **We developed a methodology to predict changes in visual performance that result from changes in the optical properties of the eye.**
• METHODS: **Exact raytracing of schematic eyes was used to calculate the point spread function and the modulation transfer function of the visual system. The Stiles-Crawford effect, photopic response, diffraction, and the retinal contrast sensitivity are included in the model. Visual acuity was predicted by examining the modulation of the resultant retinal image of a bar target and by determining when the modulation falls below a threshold value. Visual acuity was predicted for refractive errors ranging from 0 to 5 diopters and for pupil diameters ranging from 0.5 to 8 mm.**
• RESULTS: **Visual acuity predictions were compared to clinically found Snellen visual acuities and were found to be highly correlated (r^2 = .909).**
• CONCLUSIONS: **This modeling technique shows promise as a means of evaluating clinical and surgical procedures before undertaking clinical trials.**

THE GOAL OF VISUAL MODELING IS TO PREDICT the visual performance or change in visual performance of an individual from a model of the human visual system. When modeling the visual system, it is convenient to consider at least two distinct functions in the eye. The first is the production of an image incident on the retina by the optical system of the eye. The second is the conversion of this real image into a perceived image by the retina and brain. Optical acuity can be defined as a measure of the quality of the image falling onto the retina, which is completely independent of the combined functions of the retina and brain. A variety of schematic eyes have been suggested to help model the function of the eye and, in some cases, to predict optical acuity.[1-9]

Schematic eyes are simplified representations of the optical system of the eye. They have evolved from models that predict the first-order properties of biologic eyes to models that include proper aberration content or match clinically found retinal illumination. As these additional factors are included, the complexity of the model increases. Because early eye models were evaluated by hand, simpler models were adequate. High-speed computers and sophisticated software packages can now easily and quickly handle many of the complexities of more recent eye models.

Some of the earliest eye models were introduced by Gullstrand[1] and von Helmholtz.[2] These models are a series of spherical surfaces that predict the first-order properties of the eye. Gullstrand's eye model was designed to be anatomically accurate to the first order. The cornea in the model consisted of two surfaces whose spherical curvatures were obtained by studying a variety of biologic eyes. The crystalline lens is modeled as a lower index shell with a higher index core to approximate the gradient index structure of actual lenses. The drawback of this anatomically based model is that much calculation is necessary to raytrace the model. Von Helmholtz's model is simpler and assumes that the cornea is a single surface and that the lens has a uniform effective index. Le Grand and El Hage[3] similarly simplified Gullstrand's schematic eye by making the lens uniform index, but maintained the two-surface cornea. All three of these models are still relatively popular today for studying

Accepted for publication Feb. 6, 1995.
From the Optical Sciences Center (Drs. Greivenkamp and Miller, Mr. Schwiegerling, and Mr. Mellinger) and the Department of Ophthalmology (Drs. Greivenkamp and Miller), University of Arizona, Tucson, Arizona.
No reprints are available.

the first-order properties of the eye. They all, however, fail to predict the aberration content of biologic eyes. The spherical aberration of these models remains well undercorrected compared with experimental findings.[4] Lotmar[5] modified the Gullstrand-Le Grand eye model by introducing aspheric surfaces on the anterior surface of the cornea and posterior surface of the lens. The asphericity of the cornea was determined keratometrically, and the asphericity of the posterior lens surface was varied to match the measured spherical aberration. El Hage and Berny[6] produced a similar model, except that they varied the asphericity of both lens surfaces to match the measured spherical aberration. Navarro, Santamaría, and Bescós[4] introduced aspheric surfaces on the anterior and posterior surfaces of both the cornea and lens. The shapes of these surfaces were an average of clinical measurements, and the dispersions of the eye media were adjusted to give clinically measured amounts of longitudinal chromatic aberration. The Navarro model also includes the Stiles-Crawford effect in the analysis. The Kooijman[7] eye model also uses all aspheric surfaces but is based on matching measured retinal illumination patterns rather than aberration content.

Simplified schematic eyes, which are based on a corneal surface alone, have also been used to model visual performance. Camp and associates[8,9] reported a technique for predicting the optical image formed on the retina from the actual measured corneal shape of an eye. The corneal power as a function of position is measured using a commercially available corneal topographer. This corneal power map is then used as the single surface of the simplified eye model. The geometric point spread function is determined by using a paraxial ray trace. The point spread function is the image of a point of light formed by the optical system. A series of rays from an object point is traced through different locations on the cornea. With this first-order model, the amount of bending of the ray is determined by the radial position of the ray and the radial corneal power at the ray intersection. The refracted rays are then extended to the image plane with the requirement that the ray path is restricted to a plane containing the optical axis and the intersection point (a meridional plane). After tracing a sufficient number of rays, the point spread function is approximated by the ray density in the image plane. To visualize the effects of different corneal shapes, a convolution technique is used to predict the images of Snellen and variable contrast letters formed by the cornea (a perfect image of the target is blurred by the point spread function). Conditions such as keratoconus and the effects of surgical procedures, such as epikeratophakia for aphakia and radial keratotomy, have been evaluated with this method. The method shows that different types of corneal errors produce different and distinctive point spread functions, and the visual performance in the presence of such errors can be subjectively evaluated from the appearance of the Snellen letters. The model performs well for severely distorted corneal surfaces but has difficulties predicting visual performance in normal patients. The methodology outlined above can, with some refinement, be extended to include the effects of the entire visual system and not just the cornea.

All of these schematic eye models can be used to predict the optical acuity. However, to fully describe the performance of the human visual system, the combined functions of the retina and brain must also be taken into account. When the combined functions of the retina and brain are included in modeling the human visual system, the concept of optical acuity must be extended to visual acuity. Visual acuity is related to the angular size of the smallest high-contrast target an individual can recognize. It is a combination of the performance of the eye optics, retinal effects, and processing performed by the brain. Optical acuity can be inferred from the schematic eye models mentioned above. By combining the effects of the retina and brain with these models, prediction of the true visual performance can be obtained.

To build on the work of Camp and associates[8,9] to predict optical and visual acuity, it is important to understand the limitations of their paraxial model. The first limitation is that the model is first order. Under this assumption, a spherical refracting surface will have no aberrations: a point source would image to a perfect point image. Paraxial raytraces ignore the surface sag and only use the radial surface power at the ray intersection point. Exact raytracing uses Snell's law to determine the ray bending at a surface. The exact intersection point of the ray with the optical surface must be determined in three dimensions, and the surface slope or surface normal must be calculated from the actual corneal surface height. Rays are also allowed to refract out of a meridional

plane. A second limitation is that the paraxial method ignores the effects of diffraction from the pupil, which results in a point spread function with nonzero blur size even with no aberrations.[10] Diffraction is a fundamental limit on the size of the point spread function, and the effects of diffraction are most noticeable for small pupil sizes. A third limitation is the use of a simplified eye model, which removes the effects of the inherent aberrations of the eye. Camp and associates[8,9] were aware of these limitations, and the choices they made were based on the desire to reduce the computational complexity (or the computation time) of the modeling. Other effects that are not included in the raytracing method of Camp and associates are the Stiles-Crawford effect and the combined functions of the retina and brain.

In this study, we modeled and predicted visual acuity. The optical performance of a schematic eye is analyzed through the use of exact optical raytracing. The combined functions of the retina and brain are then applied to the raytrace results to make a nonsubjective visual acuity prediction. To evaluate the performance of this visual system model, visual acuity was predicted for a variety of refractive power errors and pupil sizes. The results are compared with clinical data, and a high degree of correlation is found. Finally, the limitations and possible uses of these methods are discussed.

MATERIAL AND METHODS

IN THIS STUDY, WE ATTEMPTED TO OVERCOME THE limitations of the paraxial model of Camp and associates.[8,9] We first modeled optical acuity and later extended the analysis to predict visual acuity. The modeling was based on exact raytracing and included diffraction, the Stiles-Crawford effect, and the combined functions of the retina and brain. A schematic eye with aspheric surfaces was used. We somewhat arbitrarily chose the Kooijman[7] eye model as the starting point.

Exact raytrace programs have been developed by the optical industry to aid in the design and development of optical systems. In these programs, an optical system is represented by a series of surfaces, each with a curvature and possible asphericity, spacings, and indices. From this information and a user-defined pupil size, the programs can perform an exact raytrace. The set of raytrace data can then be used to evaluate the performance of the optical system. Some of the analyses used to evaluate performance include diffraction-based point spread functions and modulation transfer functions. These point spread functions and modulation transfer functions contain much detailed information about the performance of an optical system but do not relate to the clinical measurement of visual performance in an easy or obvious fashion. A patient's subjective evaluation of his or her visual performance is based on how well he or she sees details in the image of some test target. These images are more easily and quickly interpreted than abstract mathematical functions, such as the point spread function or the modulation transfer function. If the point spread function or the modulation transfer function of the system is known, the resulting image can be calculated. Methods for obtaining the point spread function and the modulation transfer function from the exact raytrace data and their associated properties will be briefly introduced in this section. Additionally, methods for obtaining degraded images of an arbitrary object from these functions will also be considered. This material is intended as an introduction; a more thorough description can be found in the texts by Smith[10] and Goodman.[11]

Calculation of the point spread function and modulation transfer function from exact raytracing—Exact raytracing is performed by propagating rays from a given object point through a set of locations in the entrance pupil of the optical system. Each ray is extended until it intercepts the next refracting surface. Once the intersection point between the ray and the surface is found, the angle between the ray and the local surface normal is calculated. The ray is refracted using Snell's law, and the ray is propagated to the next surface. The entire process is repeated until the ray reaches the image plane. In a perfect optical system, a point would be imaged to a point; a set of rays traced through the optical system would all intersect at a single image point. In an aberrated system, the rays from different locations in the pupil intersect the image plane at different locations resulting in a blur.

A related method for analyzing optical systems uses

wavefronts. The wavefront is always perpendicular to the rays. For an aberration-free optical system, the wavefront leaving the exit pupil is perfectly spherical and converges to a point in the image plane. With aberrations, the wavefront leaving the pupil is not spherical, since the rays do not converge to a single point. The wavefront produced by an optical system is determined from the exact raytrace by calculating the optical path (product of index of refraction and distance) along each ray. The difference in these paths from ray to ray in the exit pupil is the wavefront error function. The effects of diffraction caused by the finite extent of the pupil can also be included in this wavefront picture. Both the point spread function and the modulation transfer function of the system can be calculated from a complex function whose modulus is the transmission of the pupil and whose phase is the wavefront error function. This complex function is known as the pupil function.[11]

The point spread function, also known as the impulse response, is the intensity distribution of the image of a point source.[10] It can be calculated from the scaled square modulus of the Fourier transform of the pupil function. Since diffraction is present in any real optical system, the point spread function has a minimum blur size inversely proportional to the pupil diameter. Aberrations introduced by the optical system will further blur the point image. Over a small field of view, the point spread function does not change significantly in functional form. According to this assumption, the blurred optical image is obtained by convolving the point spread function with the object. The object is modeled as an array of incoherent point sources. The effect of the convolution is to blur each point in the object by the point spread function weighted by the local object intensity. For a given object point, the corresponding image intensity will be the sum of the point spread function at that point and the contributions from the tails of the point spread functions from other points in the vicinity. The size or width of the overlapping point spread functions determines the amount of image blur. This point spread function width can be used as a measure of the performance of an optical system.

The optical transfer function of the optical system is the Fourier transform of the system point spread function and is in general a complex-valued function. The modulation transfer function is given by the modulus of this function; however, 180-degree phase shifts are often indicated in modulation transfer function plots by allowing the modulation transfer function to take on negative values. This modification is done because rotationally symmetric systems are limited to phase shifts of 0 and 180 degrees. The modulation transfer function at a particular spatial frequency measures the reduction in modulation between a sine-wave object and its image. The modulation transfer function is usually normalized to unity at zero spatial frequency and is plotted as a function of spatial frequency (of the sine wave in either object or image space). It can also be calculated directly as a scaled autocorrelation of the pupil function. The effect of the finite pupil size is to limit the maximum spatial frequency that can pass through the optical system, and this frequency is known as the cutoff frequency.[11] The modulation transfer function will be zero for all frequencies above the cutoff frequency. By using modulation transfer functions, the image of a given object through the optical system is calculated by multiplying the object spectrum by the system modulation transfer function to get the image spectrum. The blurred image is then the inverse Fourier transform of this result. This is analogous to a Fourier decomposition of the object into a set of sinusoidal patterns, each of which is reduced in modulation by the modulation transfer function.

Image formation on the retina—If the point spread function or modulation transfer function of an optical system is known, the illumination pattern in the image plane corresponding to an object can be determined. The various calculation paths and interrelationships previously described are shown in Figure 1. The goal is to predict the image from an object by using the point spread function or the modulation transfer function. Either path produces the same result, and both methods will be used in the following sections to predict visual performance.

To predict optical acuity, the point spread function or modulation transfer function of a schematic eye is needed. The surface shapes, thicknesses, and indices of the Kooijman[7] schematic eye were used to perform an exact raytrace. The point spread function or the modulation transfer function was then obtained from

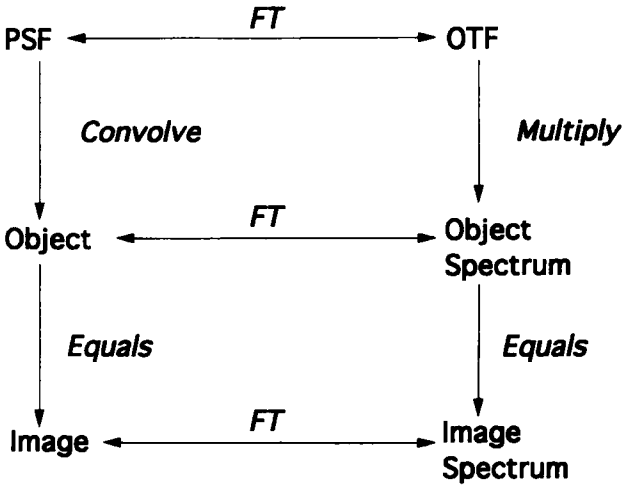

Fig. 1 (Greivenkamp and associates). Calculation methods for obtaining the image of a given object from either the point spread function (PSF) or the optical transfer function (OTF). One method is to convolve the point spread function with the object to obtain the image (left-hand column). An alternative method is to Fourier transform (FT) the point spread function and the object to obtain the optical transfer function and the object spectrum, respectively. The product of the optical transfer function and the object spectrum gives the image spectrum (right-hand column). The image is obtained by an inverse Fourier transform of the image spectrum.

the set of raytrace data. For the present analysis, Code V lens design software (Optical Research Associates, Pasadena, California) was used, although other programs have similar capabilities. As described henceforth, the Stiles-Crawford effect and the photopic response of the eye were also included in this analysis.

The Kooijman eye model used in this study is diagrammed in Figure 2, and its specifications are

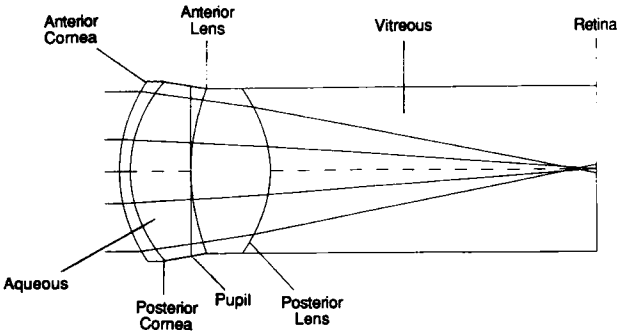

Fig. 2 (Greivenkamp and associates). The Kooijman[7] schematic eye.

given in the Table. The Table gives the radius of curvature, R, and the conic constant, K, for each of the aspheric surfaces. The surfaces can be generated in Cartesian coordinates by using the equation:

$$(1)\ z = \frac{(x^2 + y^2)\left(\frac{1}{R}\right)}{1 + \sqrt{1 - (K + 1)(x^2 + y^2)\left(\frac{1}{R}\right)^2}},$$

where x and y are the Cartesian coordinates, and z is the surface sag.[12] The thickness values refer to the vertex spacing following the surface. The indices are for the F, d, and C spectral lines and are for the medium corresponding to the spacing. Since the Kooijman model is specified only for a single wavelength, the indices for the F and C lines are taken from the eye model of Navarro, Santamaría, and Bescós.[4] (Note that there are several typographical errors in that paper. In the Hertzberger formula, the coefficients should read $a1(\lambda) = 0.66147196 - 0.40352796\,\lambda^2 - \ldots$ and $a4(\lambda) = -1.75835059 + \ldots$ The refractive index of the cornea should be 1.376.). The pupil is located at the anterior lens surface.

TABLE

SPECIFICATIONS OF THE KOOIJMAN SCHEMATIC EYE

SURFACE	ANTERIOR CORNEA	POSTERIOR CORNEA	ANTERIOR LENS	POSTERIOR LENS
Radius of curvature, R (mm)	7.8	6.5	10.2	−6.0
Conic constant, K	−0.25	−0.25	−3.06	−1.0
Shape	Ellipsoid	Ellipsoid	Hyperboloid	Paraboloid
Thickness (mm)	0.55	3.05	4.0	16.6
Index λ = 486.1 nm (F)	1.3807	1.3422	1.42625	1.3407
Index λ = 587.6 nm (d)	1.3771	1.3374	1.42	1.336
Index λ = 656.3 nm (C)	1.37405	1.3354	1.4175	1.3341

While the fovea is located several degrees from the optical axis of the eye model, visual performance is evaluated along the optical axis for simplicity and to maintain rotational symmetry. This restriction can be removed if desired. The curvature of the retina is not important for this analysis because the performance of the model is evaluated only over a small field of view.

The Stiles-Crawford effect is easily added to the raytrace model. The Stiles-Crawford effect relates a reduction in the perceived visual response as a function of increasing angles of incidence of light on the retina.[13] The Stiles-Crawford effect is included in the raytrace eye model by placing an apodizing filter in the entrance pupil of the system. An apodizing filter has a spatially varying optical transmission; in this case, the central portion of the filter will have a higher transmission than the edges.[10] As the radial distance of the ray from the optical axis in the pupil increases, the angle of incidence of the ray onto the retina also increases. The filter provides the appropriate weighting to each ray based on its position in the pupil and therefore its angle of incidence at the retina. Rays farther from the optical axis in the pupil are weighted less than axial rays, to simulate the Stiles-Crawford effect. The apodizing filter provides a gaussian falloff in transmission through the entrance pupil. The transmission, T, as a function position in the entrance pupil of such a filter, is described by van Meeteren[14] and is given by the equation:

$$(2)\ T(\rho) = e^{-\alpha\rho^2/2},$$

where ρ is the radial pupil coordinate, and $\alpha = 0.108$. The intensity transmission is unity at the center of the pupil and falls of to 0.42 at a pupil radius of 4 mm.

Even though the Stiles-Crawford effect is primarily a retinal effect, it is easy and best to model it as part of the optical system. The inclusion of the Stiles-Crawford effect in the modeling is important. For rays going through the edge of the pupil, more aberrations are introduced. By providing a lower weighting for these more eccentric rays, the Stiles-Crawford effect helps to reduce these aberrations and improve the perceived image quality. Since the Stiles-Crawford effect can markedly improve visual performance, it should be included in the model to ensure prediction accuracy. It is important to note that the modeling will now differ (at least in order) from the actual physical process occurring in the eye. As quantities such as the point spread function are computed, the modeling will not predict the optical illumination pattern on the retina, but rather a Stiles-Crawford-weighted point spread function. The same holds for other quantities.

Three wavelengths are used in the modeling. These wavelengths (λ) are 486.1, 587.6, and 656.3 nm, which correspond to the F, d, and C spectral lines, respectively, and span the approximate range of the visible spectrum. To approximate the photopic response of the eye, the central wavelength is weighted three times more heavily than the other wavelengths.

All the factors described above are entered into the lens design software, a pupil size is defined, and a set of rays is traced through the model. As described above, the diffraction point spread function or diffraction modulation transfer function is calculated. If the point spread function is generated, the optical image falling on the retina (weighted by the Stiles-Crawford effect) is obtained by convolving this optical point spread function with the scene or object (Fig. 1). The optical acuity can be observed by using an object that is a set of letters corresponding to the letter sizes on a Snellen chart.[8,9] For a given point spread function, the images of the letters will become increasingly difficult to read as they get smaller. The size at which the letter is no longer identifiable corresponds to the optical acuity. For illustration, Figure 3 shows the resultant image of a series of Snellen Es when they are convolved with a gaussian point spread function.

While the convolution method of determining a resultant retinal image is easy to visualize, it is computationally slow. The identical result can be obtained much faster by using Fourier theory and the speed of the fast Fourier transform. Fast Fourier transforms are computer algorithms for performing discrete Fourier transforms. The algorithms have been optimized for computational speed and are much faster than any convolution algorithm. As stated earlier, the Fourier transform of the point spread function gives the modulation transfer function of the optical system. An image can be obtained by first multiplying the modulation transfer function by the spectrum of an object and then inverse Fourier transforming the product. This is the alternate path shown in Figure 1. The resulting blurred image is the

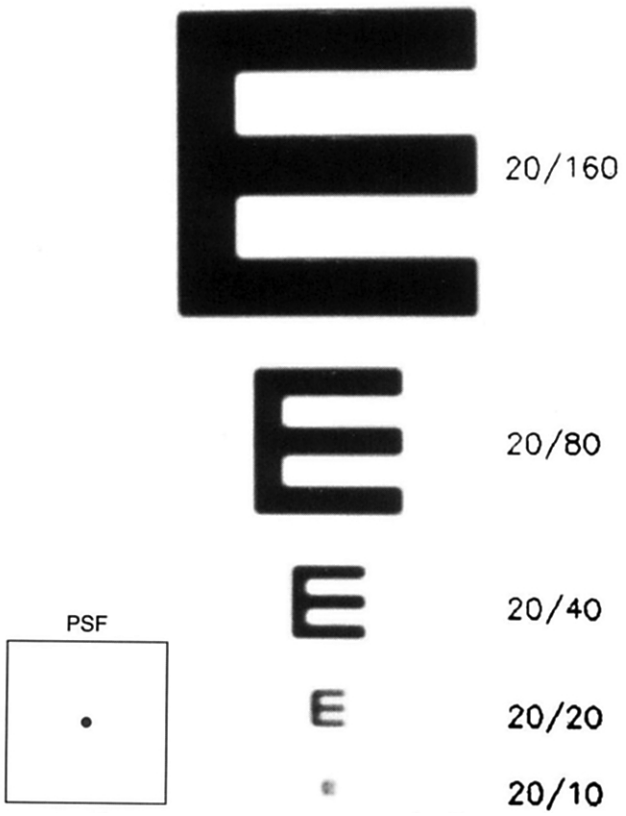

Fig. 3 (Greivenkamp and associates). Convolution of various sized Snellen Es with a gaussian point spread function. The relative Snellen acuity is shown to the right of each Snellen E. The point spread function is shown to scale in the lower left-hand corner.

same as the image obtained using the convolution technique.

The model has been used to calculate the point spread function and the modulation transfer function of the model eye as a function of refractive error and pupil diameter. To simulate a refractive error, a spectacle lens is placed at the front focal point of the eye model. The power of the spectacle lens is varied to introduce the desired amount of refractive error. To ensure that additional chromatic aberration is not introduced into the model, a dispersionless lens is used. Figure 4 shows the resulting point spread functions obtained for a 4-mm pupil with two different levels of refractive error.

The modulation transfer functions corresponding to these point spread functions were then used to blur a Snellen visual acuity chart as previously described. However, instead of displaying the E with decreasing size, we have found it easier to display each E at the same size and to vary the scale factor of the point spread function. The Snellen Es are kept a constant size (80 × 80 pixels, corresponding to 16 samples across each black bar or white space), and the size of the point spread function is changed to examine different visual acuity levels. The advantage of varying the point spread function scale instead of the Snellen letter size is that the number of samples displayed for each E remains constant. The display resolution does not become a factor in examining the degree of blur. Because this method is used, the blurred images all appear the same size, and only the scales will change between successive acuity levels. The left side of Figure 5 shows the convolution of a series of Snellen Es, with a point spread function generated from the eye model by using a 4-mm pupil and a 0.5-diopter refractive error.

To predict optical acuity, the quality of the blurred images needs to be evaluated. Image quality is, however, ambiguously defined and highly subjective. Examining the blurred images formed by the methods previously described underestimates visual performance. The visual acuities predicted subjectively from the smallest identifiable E are worse than the visual acuities found clinically for the same refractive errors and pupil sizes. To predict visual performance accurately, a more objective analysis of the image quality is needed.

Visual acuity prediction—An objective procedure for determining image quality and predicting visual acuity can be based on the modulation in the resulting image. Modulation is a well-defined quantity that is a direct measure of image quality. The right side of Figure 5 shows the intensity profiles along a vertical slice through the three bars of the Snellen E images in the left side of Figure 5. The modulation M of the image is determined from these profiles by the equation:

$$(3)\ M = \frac{I_{MAX} - I_{MIN}}{I_{MAX} + I_{MIN}},$$

where I_{MAX} is the maximum image intensity, and I_{MIN} is the minimum image intensity.[10] Because each E is a different size, the bars of each E correspond to different spatial frequencies. Figure 6 illustrates the method of determining the modulation of a sinusoidal pattern.

Fig. 4 (Greivenkamp and associates). Left, The point spread function for a 0.5-diopter refractive error and a 4-mm pupil diameter. Right, The point spread function for a 1.0-diopter refractive error and a 4-mm pupil diameter. The full dimension of each plot is 0.252 × 0.252 mm.

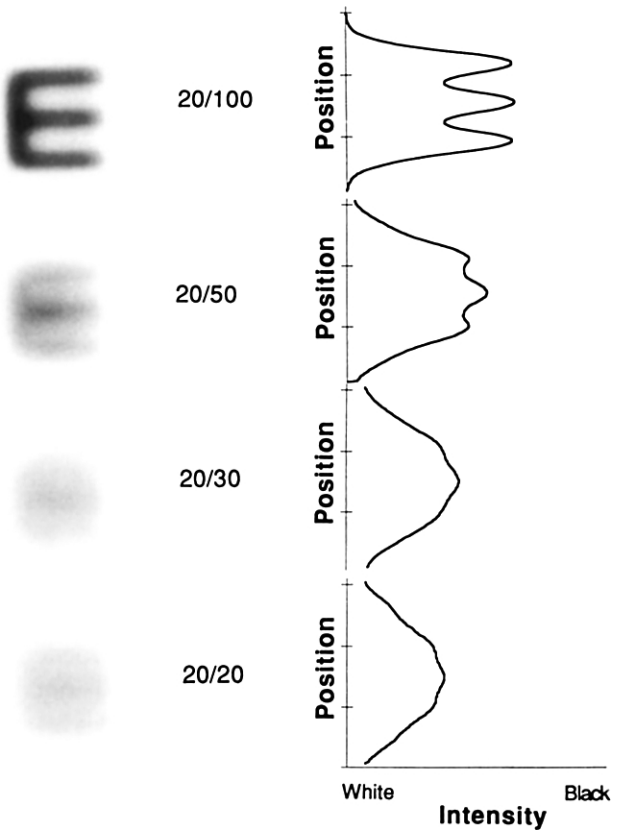

Fig. 5 (Greivenkamp and associates). Left, The image of several Snellen Es for the eye model with a 4-mm pupil and 0.5-diopter refractive error. The relative Snellen acuity is seen to the right of each blurred image. Right, A vertical intensity profile through the Snellen E to display the modulation present in the resultant images.

To accurately predict visual performance from the image modulation, the combined functions of the retina and brain must be included in the model. An available measure that fits into this framework is the contrast sensitivity function. This function describes the minimum image modulation required for a specific spatial frequency to be detected. There are several reported measures of the retinal contrast sensitivity,

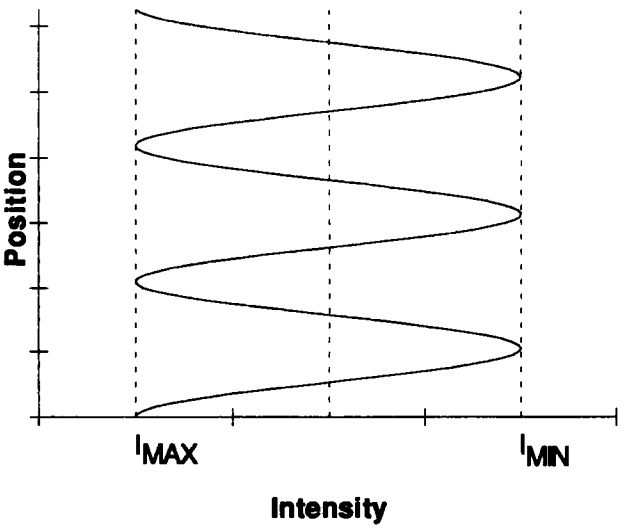

Fig. 6 (Greivenkamp and associates). A simulated intensity profile through a blurred image of a Snellen E. The brightest intensity (I_{MAX}) and the darkest intensity (I_{MIN}) are used to calculate the modulation in the blurred image.

and for this modeling, the results of Campbell and Green[15] were used. They measured the retinal contrast sensitivity function by imaging two coherent point sources near the front nodal point of the eye. Light from the two sources interferes to form a sinusoidal pattern on the retina.[16] In this arrangement, the effects of diffraction, refractive error, and aberration on the modulation and frequency of the sinusoidal pattern are negligible. The modulation of the sinusoidal pattern is varied by adding uniform-intensity incoherent illumination to the pattern on the retina. Its frequency is varied by changing the point spacing. By finding the minimum detectable modulation for various spatial frequencies, the retinal contrast sensitivity function is calculated. The retinal contrast sensitivity is the reciprocal of the minimum image contrast required on the retina to observe a particular spatial frequency. The minimum image contrast requirement is called the modulation threshold. Figure 7 shows the modulation threshold adapted from the results of Campbell and Green.[15] Because of the method of measurement, the Stiles-Crawford effect does not influence the modulation threshold, showing the need to include this effect in the eye model.

The clinical measurement of visual acuity uses some form of eye chart, such as a Snellen chart. A Snellen chart consists of a series of letters that decrease in size from line to line. When an observer views the chart, the smaller letters on the chart will be blurred the most or, equivalently, will show the greatest reduction in image modulation. The letters for which the modulation is below the threshold of the spatial frequency corresponding to that letter will not be resolved. The letter size for which the image modulation equals the threshold is an estimate of the visual acuity of the system. This modeling method for predicting visual acuity is an attempt to be completely analogous to clinical methods for a given pupil size and dioptric blur. The modulation of a blurred E computed by the raytrace model is compared with the modulation threshold of the retina, and the size of the E is varied until its image modulation equals the threshold as measured by Campbell and Green.[15] The spatial frequency of this E is related to a certain line on the Snellen eye chart and corresponds to a visual acuity. This prediction method includes the optical aberrations of the eye, diffraction, the retinal contrast sensitivity, and the Stiles-Crawford effect.

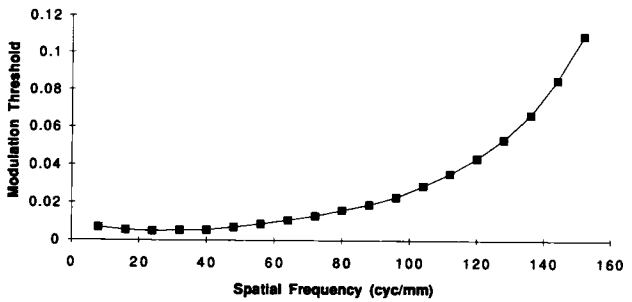

Fig. 7 (Greivenkamp and associates). Modulation threshold function of Campbell and Green.[15]

This method is simple for conceptual purposes but proves exceedingly tedious in practice. The same results once again are more easily and quickly obtained by returning to the spatial frequency domain. If the modulation threshold is plotted on the same graph as the modeled modulation transfer function, the spatial frequency where the modulation transfer function equals the modulation threshold is the maximum sinusoidal spatial frequency that can be detected by an individual. However, the test charts used to measure visual acuity use binary (that is, black and white) targets. It is easy to visualize the bars of a Snellen E as a bar target. To account for this difference in predicting visual acuity, a close relative of the modulation transfer function, the square-wave modulation transfer function,[10] can be used. The modulation transfer function describes the attenuation of a sinusoidal pattern imaged through an optical system. Similarly, the square-wave modulation transfer function describes the attenuation of a bar target imaged through an optical system. The square-wave modulation transfer function is obtained from the modulation transfer function by Fourier decomposing the bar target. A bar target is made up of a fundamental sinusoidal frequency along with various amounts of higher-order odd harmonics. Each of these harmonics along with the fundamental frequency is attenuated as it passes through the optical system. The amount of attenuation of each individual spatial frequency component of the bar pattern is deter-

mined by the modulation transfer function. The reassembled frequencies form the image of the bar target, and the net modulation of the image is the square wave response at a given frequency. Mathematically, the square-wave modulation transfer function is given by the equation:

$$(4)\ \mathrm{SMTF}(\xi) = \frac{4}{\pi}\left[\mathrm{MTF}(\xi) - \frac{\mathrm{MTF}(3\xi)}{3} + \frac{\mathrm{MTF}(5\xi)}{5} - \frac{\mathrm{MTF}(7\xi)}{7} + \ldots\right],$$

where ξ is spatial frequency, MTF is the modulation transfer function, and SMTF is the square-wave modulation transfer function. The square-wave modulation transfer function is readily available as a standard output from the raytrace code. The bars of a Snellen E can be considered to be a truncated bar target. Since visual acuity is normally measured using Snellen letters or some equivalent, matching the modulation threshold with the square-wave modulation transfer function is the appropriate choice for determining visual acuity. Figure 8 shows the square-wave modulation transfer function for the Kooijman eye model with a 2-mm pupil and a plot of the modulation threshold. The spatial frequency where the curves intersect is an estimate of the visual acuity.

Visual acuity is usually not given in terms of spatial frequency. A Snellen E is 2.5 cycles in the vertical direction and for a given line on the eye chart, the E has a certain height on the retina. If 2.5 cycles is divided by this height, the spatial frequency corresponding to the line on the eye chart (or visual acuity) is obtained. The conversion of spatial frequency to Snellen distance is given by the equation:

$$(5)\ \text{Snellen Distance} = \frac{2{,}000}{\xi},$$

where ξ is the spatial frequency, in cycles per millimeter, on the retina.[17] For example, in Figure 8 the intersection point of the square-wave modulation transfer function and the modulation threshold occurs at ξ = 155 cycles/mm. The equivalent Snellen distance is 13, or the visual acuity is 20/13.

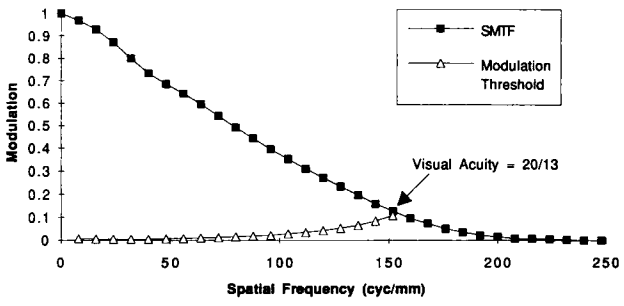

Fig. 8 (Greivenkamp and associates). Determination of visual acuity from the square-wave modulation transfer function (SMTF). The intersection of the square-wave modulation transfer function and the modulation threshold at 153 cyc/mm determines the spatial frequency of a barely resolvable bar target. This spatial frequency can be converted to an angular subtense or a Snellen distance.

RESULTS

THE CLINICAL DATA USED TO TEST THE VALIDITY OF THIS method of visual acuity prediction are those of Holladay and associates.[18] They provide a literature summary of the clinical relationship between Snellen acuity, best-corrected refractive error, and pupil diameter. The summary results are shown in Figure 9. These results combine 12 studies, each with ten to 10,000 patients. The results of this survey are intuitively pleasing. They show that, for small pupil sizes, diffraction is the primary limitation in visual acuity and that refractive error is not appreciable. As the pupil diameter increases to 3 to 4 mm, visual acuity also improves; here diffraction only slightly degrades

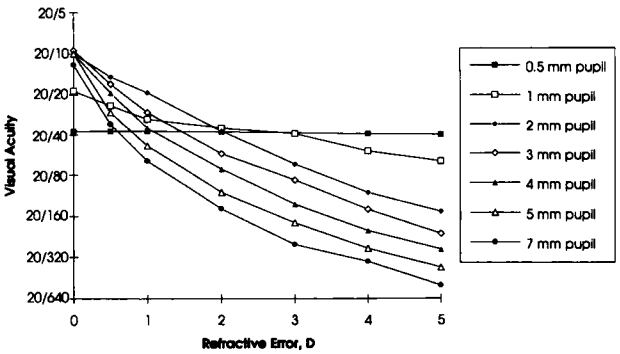

Fig. 9 (Greivenkamp and associates). Visual acuity vs refractive error in diopters (D) and pupil diameter. Each visual acuity value is from a summary of clinical results compiled by Holladay and associates.[18]

the image while aberrations are still minimal. Increasing the pupil diameter further causes a falloff in visual acuity as aberrations begin to markedly affect image quality. Increasing power error steadily diminishes acuity for these final two cases. Since the Holladay results are so well behaved and are an average of thousands of patients, they are taken as accurate predictions of visual acuity for individuals with normal retinal contrast sensitivities.

For each power error (0, 0.5, 1, 2, 3, 4, and 5 diopters) and pupil size (0.5, 1, 2, 3, 4, 5, 6, 7, and 8 mm) presented in the clinical summary, the corresponding schematic eye was modeled. Only myopic refractive errors were examined. The entrance pupil was set to the desired diameter, and the power of the spectacle lens placed at the front focal point of the eye was varied to introduce the appropriate amount of refractive error. From the resulting raytrace, the square-wave response was generated for each of the 63 combinations of pupil size and power error, and the intersection of the square-wave modulation transfer function and the modulation threshold was found. The intersection was converted to a Snellen visual acuity. Figure 10 shows the results of the visual acuity predictions from the eye model.

By comparing Figure 10 directly to Figure 9, the model results followed the same general trend as the survey by Holladay and associates.[18] Figure 11 shows a plot of the visual acuity for the clinical data vs the modeling results. There was a strong linear correlation (r^2 = .909), and all the modeling predictions fell within one octave of acuity of the clinical results.

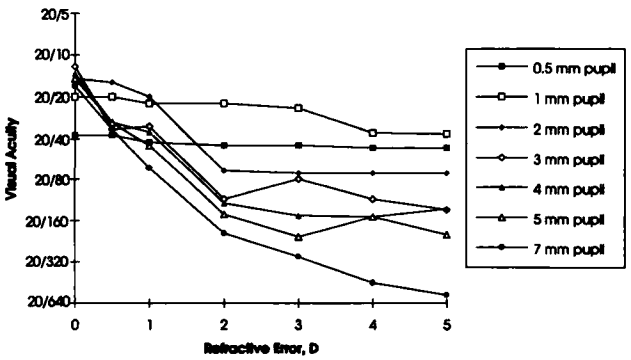

Fig. 10 (Greivenkamp and associates). Visual acuity vs refractive error in diopters (D) and pupil diameter. Each visual acuity value is predicted from the eye model.

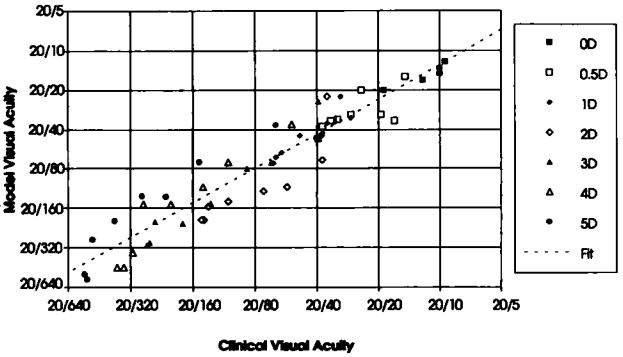

Fig. 11 (Greivenkamp and associates). Plot of the clinical visual acuity results vs the visual acuities predicted from the eye model. The refractive errors are measured in diopters (D) and range from 0 to 5 diopters. The dashed line represents a linear fit to the data, and the correlation coefficient, r^2, is 90.9%.

The diffraction-limited data points were calculated by finding the maximum spatial frequency that can pass through an ideal optical system. These data points were neither a consequence of the specific modeling techniques described above nor measured clinically in the studies compiled by Holladay and associates.[18] These data points were not included in the statistical analysis.

DISCUSSION

IN THIS STUDY, WE ATTEMPTED TO MODEL THE HUMAN visual system to predict visual performance. We used a modeling methodology that included as many clinically relevant properties as possible. These factors included the Stiles-Crawford effect, which reduces the influence of aberrations at large pupil sizes; the photopic response of the retina, which allows chromatic effects to be included; and the retinal contrast sensitivity function, which brings the retinal modulation threshold into the analysis. Most of these features were not addressed in earlier modeling studies. Starting with a schematic eye and an exact raytracing capability, we showed how to include these features in a straightforward manner by using commercially available optical design software. Although a number of specific functional forms have been somewhat arbitrarily assumed in this study (for example, schematic eye design, contrast sensitivity function, and the like), the methodology remains general. A differ-

ent eye model or response function can be easily substituted in the methodology.

The analysis quantitatively predicts visual performance rather than subjectively evaluates blurred images of Snellen charts (which tends to predict worse visual acuity). By including the combined functions of the retina and brain response, a more accurate prediction of visual acuity was obtained. Although important differences between our modeling results and the corresponding clinical data exist, the model does show a performance falloff with changes in refractive error and pupil size that is consistent with the clinical data. The modeling method should therefore be very useful for examining changes in visual acuity when small perturbations are applied to the model. Additionally, changes in the overall visual contrast sensitivity function can be predicted by looking at the Stiles-Crawford weighted modulation transfer functions before and after a perturbation to the eye model.

Although the model is relatively simple to implement, care must be taken when calculating the pupil function. In the presence of large amounts of aberration or refractive error, the wavefront leaving the exit pupil deviates markedly from a sphere. Only a finite number of rays are used to raytrace the optical system, and the wavefront error function is evaluated in the pupil only along these rays. If the sample density in the wavefront error array is insufficient to represent the wavefront error function, then there will be appreciable error in the point spread function or the modulation transfer function. For the point spread function or modulation transfer function to be calculated accurately, the wavefront error between adjacent points in the array must be less than one half the wavelength of light. If this condition is not met, aliasing occurs in the fast Fourier transform algorithm.[19] For the most severe cases of refractive error and pupil sizes examined in this study, the number of samples needed across the diameter of the exit pupil is several thousand. The large number of samples produces some difficulties because of long computation times and the amount of computer memory required. Work is underway to refine the modeling of the wavefront error function to ensure calculation accuracy.

A major limitation to the modeling of visual performance occurs in the presence of large amounts of aberration or refractive error. In this situation, the square-wave modulation transfer function tends to oscillate, resulting in multiple spatial frequencies where the response drops to zero. This condition can result in a contrast reversal of the image. Contrast reversal, or spurious resolution, is known to be a common consequence in defocused systems.[11] The square-wave modulation transfer function with multiple zeroes can drop below the retinal modulation threshold only to exceed the required modulation at a higher spatial frequency. This ambiguity in the threshold spatial frequency can repeat several times, resulting in several possible values for the predicted visual acuity. When this situation was encountered in this study, the frequency at which the square-wave modulation transfer function drops below the modulation threshold for the second time was chosen to represent the resolution limit. This choice permits a single contrast reversal and ignores additional reversals. Better methods for accurately determining the resolution limit in these cases are also being investigated.

The prediction accuracy of the model may be improved by obtaining response functions that are more clinically representative than those used. The retinal contrast sensitivity function of Campbell and Green[15] was assumed. The Campbell and Green data, however, are based on the measurement of a single individual at a single wavelength. Retinal contrast sensitivity varies significantly from person to person, so a contrast sensitivity norm may be needed instead. The functional form of the Stiles-Crawford attenuation may also need to be altered. The modeling of chromatic effects by evaluating the system at only three specific wavelengths may be insufficient for accurate analysis.

There may also be important ramifications resulting from the choice of the schematic eye on the performance of the model. The Kooijman[7] eye model was designed to give the clinically found retinal illumination, but its aberration content may not sufficiently match clinical measurements. Although matching all the anatomic properties of the human eye is desirable, the important goal for the schematic eye used for the modeling is that its performance matches the performance of the human eye. The least complex model that meets this requirement will minimize the computational complexity. The indices

of the aqueous, vitreous, and cornea are generally accepted as accurate representations of normal biologic eyes. The external corneal shape can be measured keratometrically. The useful parameters that remain are the shapes of the lens surfaces and the dispersion of the eye media (especially the lens).

A basic assumption of this study in predicting visual acuity is that the detection of modulation of a letter is equivalent to the recognition of that letter. This assumption may be accurate for letters such as E, when viewing conditions are great, but may be highly inaccurate for other letters or when contrast reversals exist. More sophisticated methods of determining the point on the square-wave modulation transfer function that corresponds to the visual acuity may be needed. Additionally, only rotationally symmetric optical systems have been considered to date. When errors such as astigmatism are present in the eye, the square-wave modulation transfer function curve will change with orientation. A decision process that allows a single visual acuity number to be generated must be found.

This modeling method can be used to determine the effects of clinical and surgical techniques on visual performance. Contact lens or intraocular lens performance can be evaluated, and the effects of tilt and decentration of these elements on visual acuity, modulation transfer function, or contrast sensitivity can be studied. It should be possible to model surgical procedures such as radial keratotomy and photorefractive keratectomy by altering the shape of the model cornea, raytracing the system, and examining the change that occurs in the modulation transfer function or the contrast sensitivity. The versatility and simplicity of the model are appealing. The use of modeling of this type should allow the determination of tolerances for some procedures before extensive clinical trials are undertaken.

An advantage to this type of modeling may be in the screening of new procedures. The model can be used before clinical studies, to predict the results expected from these new procedures and to eliminate studies that are not beneficial. Once a technique is verified through modeling, a clinical study can then be performed.

With some lens design software, it is possible to apply an arbitrary surface height map to any surface in the eye model. By taking advantage of this feature, corneal topography data can be incorporated into the modeling. Several commercial topographers output a surface height map of the topography data directly. By altering the corneal shape in the eye model to the surface described by these height data, clinically measured topography can be included in the visual modeling.

The modeling can also be used to predict visual performance on an individual basis. Currently, work is underway to measure corneal topography, axial length, best refraction, contrast sensitivity, and visual acuity of individuals. A customized eye model will then be constructed for that individual, and its performance and relevant anatomic features will be consistent with those of the patient. The same prediction accuracy as the modeling above is anticipated. Modifications can then be made to this custom model to simulate the postoperative performance of the individual. With this method, the effectiveness of the treatment can be evaluated ahead of time. The model potentially provides a quick and cost-effective evaluation of new and existing clinical and surgical techniques.

This work is a preliminary attempt to provide a comprehensive analysis of the human visual system to predict visual performance. The Kooijman[7] eye model was chosen as a starting point for the modeling, and additional effects, such as the Stiles-Crawford effect, diffraction, and the photopic response of the eye, were included. Exact raytracing has been used to avoid limitations of paraxial raytracing and to ensure the accuracy of the calculated point spread functions and modulation transfer functions needed to make visual acuity prediction. The prediction of visual acuity from the optical performance of the eye model requires the inclusion of the retinal contrast sensitivity function. A simple retina and brain response model is used in this work so that the methodology is easily implemented. The model's usefulness appears to be in determining the changes in visual performance caused by changes in the optical system. The results of this model were verified against clinically found results, and a high correlation ($r^2 = .909$) was found. The results of the modeling are very encouraging but show the need for additional sophistication and new approaches. The primary limitation to our methods is the calculation of the square-wave response in the presence of large aberrations.

Although the inclusion of many of the practical properties of the human visual system may appear to result in a very complex model, it is relatively simple to implement with commercially available lens design software. This modeling technique shows promise as a nonsubjective method for determining visual acuity and a quick and inexpensive means of evaluating clinical and surgical procedures.

REFERENCES

1. Gullstrand A. Appendices to part I. In: von Helmholtz H. Physiological optics, 3rd ed. Volume 1. Hamburg: Voss, 1909:350–8.
2. von Helmholtz H. Physiological optics, 3rd ed. Volumes 1 and 2. Hamburg: Voss, 1909:91–121.
3. Le Grand Y, El Hage SG. Physiological optics. Berlin: Springer-Verlag, 1980:57–69.
4. Navarro R, Santamaría J, Bescós J. Accommodation-dependent model of the human eye with aspherics. J Opt Soc Am A 1985;2:1273–81.
5. Lotmar W. Theoretical eye model with aspherics. J Opt Soc Am 1971;61:1522–9.
6. El Hage SG, Berny F. Contribution of the crystalline lens to the spherical aberration of the eye. J Opt Soc Am 1973;63:205–11.
7. Kooijman AC. Light distribution on the retina of a wide-angle theoretical eye. J Opt Soc Am 1983;73:1544–50.
8. Camp JJ, Maguire LJ, Cameron BM, Robb RA. A computer model for the evaluation of the effect of corneal topography on optical performance. Am J Ophthalmol 1990;109:379–86.
9. ———. An efficient ray tracing algorithm for modeling visual performance from corneal topography. In: Proceedings of the First Conference on Visualization in Biomedical Computing, Atlanta, Georgia, May 22–25. Piscataway, New Jersey: IEEE, 1990.
10. Smith WJ. Modern optical engineering, 2nd ed. New York: McGraw-Hill, 1990:327–63.
11. Goodman JW. Introduction to Fourier optics. New York: McGraw-Hill, 1968:101–40.
12. Malacara D, editor. Optical shop testing. New York: John Wiley & Sons, 1992:743–53.
13. Stiles WS, Crawford BH. The luminous efficiency of rays entering the eye pupil at different points. Proc R Soc Lond [Biol] 1933;112:428–50.
14. van Meeteren A. Calculations on the optical modulation transfer function of the human eye for white light. Opt Acta 1974;21:395–412.
15. Campbell FW, Green DG. Optical and retinal factors affecting visual resolution. J Physiol 1965;181:576–93.
16. Saleh BEA. Optical information processing and the human visual system. In: Stark H, editor. Applications of optical Fourier transforms. London: Academic Press, 1982:431–61.
17. Miller D. Optics and refraction. New York: Gower; 1991.
18. Holladay JT, Lynn MJ, Waring GO III, Gemmill M, Keehn GC, Fielding B. The relationship of visual acuity, refractive error, and pupil size after radial keratotomy. Arch Ophthalmol 1991;109:70–6.
19. Juergens RC, editor. Code V reference manual, Version 7.60. Volumes 1 and 2. Pasadena: Optical Research Associates, 1994.